Multipactor Discharge on a Dielectric

R. A. Kishek* and Y. Y. Lau†

Department of Nuclear Engineering and Radiological Sciences, University of Michigan, Ann Arbor, Michigan 48109-2104

(Received 14 April 1997)

This paper proposes a novel theory of single-surface multipactor discharge on a dielectric, such as an rf window. Using a Monte Carlo simulation, we obtain the susceptibility diagram, applicable to a wide range of materials, in terms of the rf electric field and of the dc electric field that may result from dielectric charging. The electron multiplication mechanism assumes realistic yield curves of secondary electrons, including distributions of emission velocities and angles for these electrons. The susceptibility diagram thus constructed allows an immediate assessment of the range of rf power over which multipactor may be expected to occur. A simple analytic theory is constructed to explain the simulation results. [S0031-9007(97)04847-3]

PACS numbers: 84.40.Zc

Multipactor discharge is a ubiquitous phenomenon observed in a multitude of devices that employ microwaves [1]. In the worst scenario, its presence leads to destruction of ceramic rf windows [2–5], erosion of metallic structures, melting of internal components, and perforation of vacuum walls [1]. Multipactor may occur when a metallic gap or a dielectric surface is exposed to an ac electric field under some favorable conditions, and its avoidance has been a major concern among workers on high power microwave sources [6], rf accelerators [4,5], and space-based communication systems [7].

Among the few publications on the theory of multipactor, the type of discharge that has been analyzed most is the two-surface multipactor [1,8–11], with even fewer publications on single-surface multipactors. Virtually all of these theories assume an rf electric field normal to the surface. They are not applicable to a dielectric surface, as in the case of an rf window, where a significant rf electric field can lie parallel to that surface.

In this paper, we present a theory of single-surface multipactor discharge on a dielectric, significantly extending the only existing theoretical treatment [2] on this subject known to us. We shall evaluate the combined action of an rf electric field that is parallel to the dielectric surface, and of a dc electric field normal to the surface that will be present if the dielectric accumulates any charge. This surface charging has been experimentally verified in a variety of situations [2–4,12]. We shall compute the multipactor growth, using realistic yield curves of secondary electron emission. A Monte Carlo simulation is performed, using empirical data as input, to account for the distributions of the emission velocities and emission angles of the secondary electrons. We ignore the space charge effects, rf loading by the multipactor, and the saturation mechanism (if any).

The geometry for this type of single-surface multipactor is shown in Fig. 1. Electrons emitted with a random velocity v_0 and a random angle ϕ with respect to the positive y axis are subjected to forces imposed by the electric fields. The dc electric field E_{dc} does not impart any energy to the electrons but simply bends back their trajectory to strike the surface at a later time. The rf electric field, of magnitude E_{rf0} and frequency ω, acts only in the y direction (parallel to the surface) and imparts energy to the multipactor electrons, as well as translates them along the y axis. Having gained energy from the rf, the electron strikes the surface with much larger energy, and, therefore, emits a number of secondary electrons by the process of secondary electron emission [13]. These secondaries also leave the surface and strike back at a later time, gaining energy in the process. If the conditions are such that there is a net gain in the number of electrons, eventually a large amount of energy gained from the rf electric field will be deposited on the surface, possibly leading to surface damage or breakdown.

The average number of secondary electrons emitted for each primary electron, called the secondary electron yield δ, is a function of the impact energy of the primary electron E_i and the angle to the normal ξ at which it strikes the surface [13,14]. The dependence of yield on impact energy is qualitatively similar for most materials, and has been fitted empirically by Vaughan [14] in a formula that depends mainly on the maximum yield $\delta_{\max}$ and the energy at which it occurs, $E_{\max}$ (Fig. 2). These two parameters are material dependent. We specify them and adopt Vaughan's formula for secondary yield to initiate the Monte Carlo simulations. Two values of impact energy, termed the first and second crossover

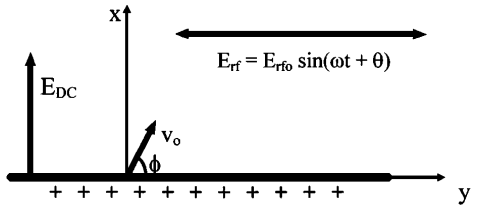

FIG. 1. Model of a single-surface multipactor in a parallel rf and normal dc electric fields.

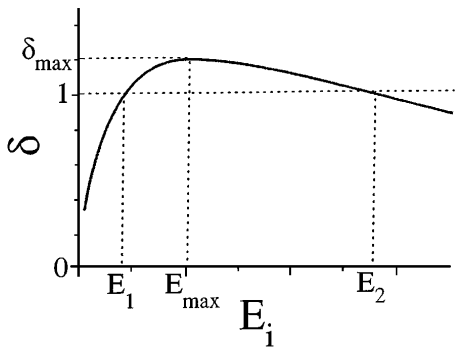

FIG. 2. Dependence of secondary electron yield on impact energy.

points, E_1 and E_2, respectively, result in a yield of 1, with $\delta > 1$ in between (Fig. 2). For impact at an angle, the parameters $E_{\max}$ and $\delta_{\max}$ are adjusted in calculating the yield, according to the following equations [14]:

$$E_{\max} = E_{\max 0}\left(1 + \frac{k_s \xi^2}{\pi}\right),$$
$$\delta_{\max} = \delta_{\max 0}\left(1 + \frac{k_s \xi^2}{2\pi}\right). \quad (1)$$

Here, $E_{\max 0}$ and $\delta_{\max 0}$ are the parameters for an impact angle of 0° (i.e., normal to the surface), and k_s is a surface smoothness factor ranging from 0 for a rough surface to 2 for a polished surface. In this paper, we set $k_s = 1$, representing a typical dull surface [14]. It is worth noting that in this situation, since the electrons gain their energy from the parallel rf, most impacts will be at almost grazing incidence ($\xi \approx \pi/2$).

To estimate the growth rate of the multipactor discharge, we follow the trajectory of a weighted macroparticle over a large number of impacts in a Monte Carlo simulation. Each time a macroparticle leaves the surface, we assign it a random initial energy $E_0 = \frac{1}{2} m v_0^2$ (m is the electron mass) and angle ϕ, according to the following distributions:

$$f(E_0) = \frac{E_0}{E_{0m}^2}\, e^{-E_0/E_{0m}}, \quad (2a)$$
$$g(\phi) = \frac{1}{2}\sin\phi\,, \quad (2b)$$

where E_{0m} is the peak of the distribution of emission energies. Note that the expected value of E_0 is $2E_{0m}$, and that $\int g(\phi)\, d\phi = 1$ over $0 < \phi < \pi$. Since the secondaries are typically emitted with energies of the order of the work function of the material [13,14], we set E_{0m} in this analysis to $0.005 E_{\max 0}$ (i.e., 2 eV for $E_{\max 0} = 400$ eV; see Table I).

An electron launched at $t = 0$ from the surface at $y = 0$ with a velocity v_0 and an angle from the positive y axis, ϕ, according to the distribution in Eq. (2), experiences a force due to the rf electric field, $E_{\mathrm{rf}0}\sin(\omega t + \theta)$. We assume the initial phase θ of the rf to be uniformly distributed. Solving the equations of motion for the electron gives

$$E_{ix} = \frac{1}{2} m v_0^2 \sin^2\phi$$
$$E_{iy} = \frac{1}{2m}\left(\frac{eE_{\mathrm{rf}0}}{\omega}\right)^2 \left\{\cos\left[\frac{2mv_0\sin\phi}{e(E_{\mathrm{dc}}/\omega)} + \theta\right] - \cos(\theta) + \frac{mv_0\cos\phi}{e(E_{\mathrm{rf}0}/\omega)}\right\}^2, \quad (3)$$

where E_{ix} and E_{iy} are the x and y components, respectively, of the impact energy. The impact angle is then

$$\xi = \arctan\left(\sqrt{\frac{E_{iy}}{E_{ix}}}\right). \quad (4)$$

Given the impact energy and angle, the yield is determined from Vaughan's empirical formula [14] mentioned above.

We use this value of the yield to adjust the charge on the macroparticle, then emit it again with a random velocity. Observing the time evolution of the charge on the macroparticle over a sufficiently long time, we can see either an exponentially growing or an exponentially decaying trend, depending on the external parameters chosen ($E_{\mathrm{dc}}, E_{\mathrm{rf}0}$, and $\delta_{\max 0}$). Hence, the simulation results in a time average over the random distributions rather than an ensemble average. To illustrate, we pick the case $\delta_{\max 0} = 2.0$, typical for some glasses used in rf windows (Table I). We then systematically vary both E_{dc} and $E_{\mathrm{rf}0}$, and, for each point on the $(E_{\mathrm{dc}}, E_{\mathrm{rf}0})$ plane, we can determine the exponential growth rate (in e folds per bounce). A positive rate indicates growth and a negative one decay. A rate of zero identifies a point on the boundary of the

TABLE I. Typical secondary electron emission parameters for materials commonly used in rf windows (adapted from Ref. [13]).

Material	$\delta_{\max 0}$	$E_{\max 0}$ (eV)	$E_1/E_{\max 0}$	$E_2/E_{\max 0}$
			(Grazing incidence)	
Al_2O_3 (alumina)	1.5–9	350–1300	0.23–0.011	10.2–24.5
Quartz-glass	2.9	420	0.072	15.6
Pyrex	2.3	340–400	0.107	13.7
Technical glasses	2–3	300–420	0.136–0.068	12.6–15.9
SiO_2 (quartz)	2.4	400	0.099	14.1

multipactor region. This information is displayed in the form of a contour plot for the case $\delta_{\max 0} = 2.0$ in Fig. 3. The contour in bold (labeled "0") is the boundary of the multipactor region.

Figure 4 shows the boundary regions for selected values of $\delta_{\max 0}$, corresponding to typical materials used in rf windows (see Table I). This set of curves applies to a wide range of dielectric materials and provides a good indication whether multipactor is to be expected or not. A glance at Fig. 4 indicates the range of rf power over which the window may be subject to multipactor. If the design parameters lie within the multipactor boundaries (positive growth rate), then multipactor is possible and the design needs to be modified. Note the wide range of parameters over which multipactor on a dielectric is possible (in contrast to the narrow range in metals [1]). Thus, dielectric materials are much more susceptible to multipactor than metals.

Following is the physical explanation for the shape of the susceptibility curves (Fig. 4). For any given values of the fields, the growth rate is determined by the average value of the secondary electron yield, averaged over the random emission energy and angle distributions [Eqs. (2a) and (2b)]. Changing the magnitude of the rf electric field changes the amount of energy the electron gains. Changing the dc field changes the amount of time spent in flight, and, hence, also the amount of energy gained. Notice from Fig. 2 that the secondary electron yield is above unity only for impact energies in between the two crossover points. If the rf electric field is too high or too low, then the amount of energy gained will vary accordingly, and, thus, the impact energy will fall outside of this region, where $\delta < 1$. This explains the existence of upper and lower boundaries. Preist and Talcott mention experimental evidence for the existence of the lower bound ($E_{\mathrm{rf\,min}}$) and predict the existence of an upper bound ($E_{\mathrm{rf\,max}}$) [2]. Furthermore, if the dc field is increased, the electron spends less time in flight, and so the rf electric field must be increased to maintain the same impact energy and yield. Notice also from Fig. 4 that the multipactor region widens with increasing $\delta_{\max 0}$, since that implies a wider range of impact energies with yields above 1.

The preceding physical understanding of the phenomenon is useful in constructing an analytic solution for the susceptibility curve boundaries. The key to obtaining a simple analytic solution is to assume that, at the two crossover points E_1 and E_2, the secondary electron yield curve (Fig. 2) is approximately linear with variation of impact energy. Under that assumption, an average impact energy equal to E_1 or E_2 corresponds to an average yield of unity. Thus, we can average the impact energy over the distribution of emission velocities and angles as well as over a uniform distribution of rf phases, θ, to obtain the expected value. Setting that average impact energy equal to E_1 or E_2 yields an equation for the boundary ($E_{\mathrm{rf}0}$ as a function of E_{dc}).

The process of averaging over the random emission velocities and angles is quite tedious, yields complicated solutions, and, hence, does not possess much of an advantage over the Monte Carlo method. The technique can be considerably simplified, however, if we assume *all* electrons are emitted *normal* to the surface, with a *single* energy equal to the average energy of the emission energy distribution ($E_0 = 2E_{0m}$). As will be seen, this drastic approximation does not qualitatively change the solution, and provides us with further insights. Hence, substituting $E_0 = 2E_{0m}$ and $\phi = 90°$ into Eq. (3), averaging over θ, and setting the resulting average impact energy equal to E_1, then E_2, we obtain the following equations for the

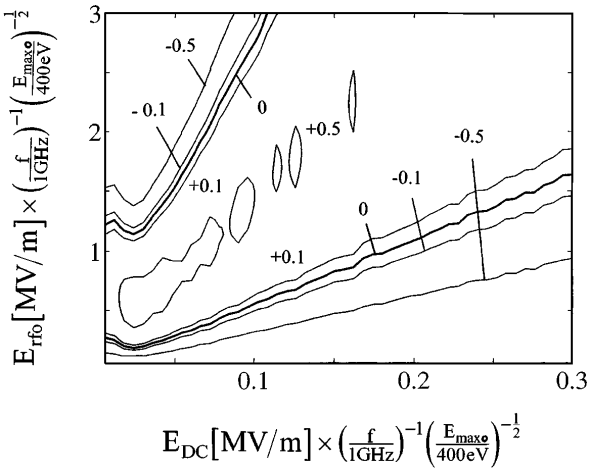

FIG. 3. Contour plot of growth rates, in units of Np/bounce, in the plane of $(E_{\mathrm{dc}}, E_{\mathrm{rf}0})$ for $\delta_{\max 0} = 2.0$, as provided by Monte Carlo simulation, assuming $E_{0m}/E_{\max 0} = 0.005$.

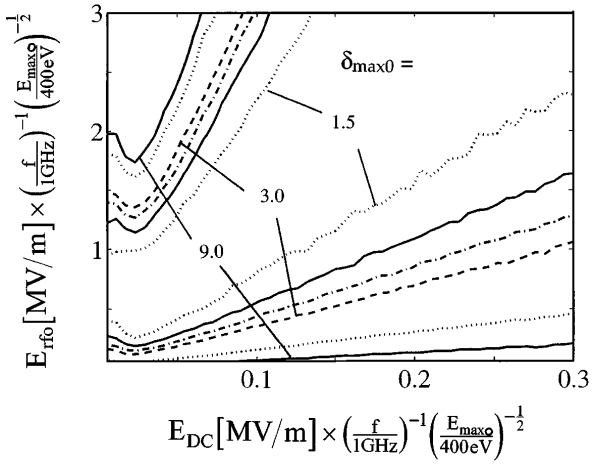

FIG. 4. Composite plot of multipactor region boundaries in the plane of $(E_{\mathrm{dc}}, E_{\mathrm{rf}0})$ for various values of $\delta_{\max 0}$ (from the innermost boundaries, $\delta_{\max 0} = 1.5$, 2.0, 2.5, 3.0, 6.0, and 9.0), assuming $E_{0m}/E_{\max 0} = 0.005$.

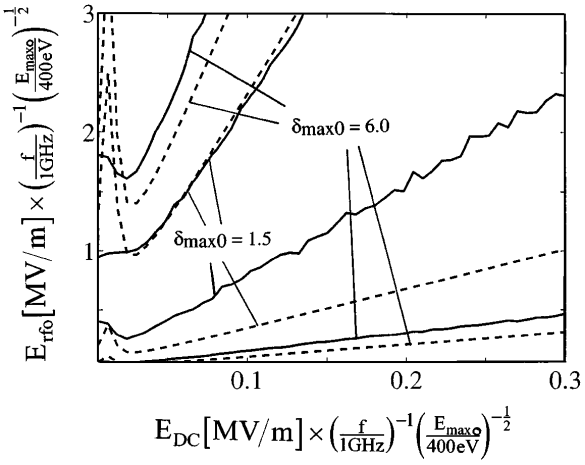

FIG. 5. Multipactor regions derived analytically (dashed) compared with the ones obtained through Monte Carlo simulations (solid) for $\delta_{\max 0} = 1.5$ and $\delta_{\max 0} = 6.0$. Here, $E_{0m}/E_{\max 0} = 0.005$.

lower and upper boundaries, respectively:

$$\frac{eE_{\text{rf min}}}{\omega\sqrt{mE_{\max 0}}} = \sqrt{\frac{2E_1/E_{\max 0}}{1 - \cos\left(\frac{4\omega\sqrt{mE_{0m}}}{eE_{\text{dc}}}\right)}}, \tag{5a}$$

$$\frac{eE_{\text{rf max}}}{\omega\sqrt{mE_{\max 0}}} = \sqrt{\frac{2E_2/E_{\max 0}}{1 - \cos\left(\frac{4\omega\sqrt{mE_{0m}}}{eE_{\text{dc}}}\right)}}. \tag{5b}$$

These boundaries are compared in Fig. 5 to the ones obtained from Monte Carlo simulations. As can be seen, the agreement is reasonably good for three out of the four cases studied [15]. The slopes of the curves in Fig. 5, in the limit of large E_{dc}, are $\frac{1}{2}\sqrt{E_{1,2}/E_{0m}}$, as easily deduced from Eqs. (5a) and (5b). Since impact is close to grazing, $\xi = \pi/2$, the values of E_1 and E_2 for grazing incidence should be used in Eqs. (5a) and (5b) (these values are listed for some materials in Table I).

In conclusion, the model and simulations presented in this paper provide us with a theoretical framework for predicting multipactor occurrence in windows and other dielectrics, perhaps for the first time. The insight provided paves the way of treating saturation due to space charge forces or rf loading, which will be addressed in a future publication [16]. The universal curve thus constructed (Fig. 4), in addition to being a useful design tool, alerts us to the wide range of parameters over which multipactor threatens dielectrics. This is in contrast to the narrow range of multipactor in metals, which are more sensitive to a resonance condition. Furthermore, the multipactor electrons in a dielectric impact the surface at grazing angles, resulting in much higher secondary electron yields. All of these, together with the poor heat conduction in a dielectric, perhaps partially explain the well-known, but inadequately understood, vulnerability of ceramic windows to rf breakdown.

We acknowledge Professor Ronald Gilgenbach and Agust Valfells for many valuable discussions. We also thank Amadi Nwakanpa and Ghassan Shahin for computation support. This work was supported by the Multidisciplinary University Research Initiative (MURI), managed by the Air Force Office of Scientific Research and subcontracted through Texas Tech University, by the Department of Navy Grant No. N00014-97-1-G001 issued by the Naval Research Laboratory, and by the Northrop Grumman Industrial Affiliates Program.

*Present address: Institute for Plasma Research, University of Maryland, College Park, MD 20742.
Electronic address: ramiak@ipr.umd.edu
†Electronic address: yylau@umich.edu

[1] J. R. M. Vaughan, IEEE Trans. Electron Devices **15**, 883 (1968); **35**, 1172 (1988).
[2] D. H. Preist and R. C. Talcott, IRE Trans. Electron Devices **8**, 243 (1961).
[3] J. R. M. Vaughan, IEEE Trans. Electron Devices **8**, 302 (1961).
[4] Robert Rimmer, Ph.D. dissertation, University of Lancaster, England, 1988.
[5] S. Yamaguchi, Y. Saito, S. Anami, and S. Michizono, IEEE Trans. Nucl. Sci. **39**, 278 (1992).
[6] C. Armstrong, J. Benford, K. Hendricks, and T. Spencer (private communication).
[7] N. Rozario *et al.*, IEEE Trans. Microwave Theory Tech. **42**, 558 (1994).
[8] S. Riyopoulos, D. Chernin, and D. Dialetis, Phys. Plasmas **2**, 3194 (1995); IEEE Trans. Electron Devices **44**, 489 (1997); S. Riyopoulos, Phys. Plasmas **4**, 1448 (1997).
[9] R. Kishek and Y. Y. Lau, Phys. Rev. Lett. **75**, 1218 (1995); Phys. Plasmas **3**, 1481 (1996).
[10] R. A. Kishek, Y. Y. Lau, and D. Chernin, Phys. Plasmas **4**, 863 (1997), and references therein.
[11] R. A. Kishek, Ph.D. thesis, University of Michigan, Ann Arbor, 1997.
[12] L. Phillips, J. Massomer, and V. Nguyen, in Proceedings of the IEEE Particle Accelerator Conference, Vancouver, 1997 (IEEE, Piscataway, NJ, to be published).
[13] O. Hachenberg and W. Brauer, *Secondary Electron Emission from Solids*, edited by L. Marton, Advances in Electronics and Electron Physics Vol. XI (Academic Press, New York, 1959), pp. 413–499.
[14] J. R. M. Vaughan, IEEE Trans. Electron Devices **36**, 1963 (1989); A. Shih and C. Hor, IEEE Trans. Electron Devices **40**, 824 (1993); C. K. Birdsall and W. B. Bridges, *Electron Dynamics of Diode Regions* (Academic Press, New York, 1966).
[15] The discrepancy in the lower curves in Fig. 5 can be attributed primarily to the assumption of normal emission in the derivation of Eq. (5). Emission at angle implies a shorter transit time, and, therefore, requires a higher rf field to supply the necessary energy to reach E_1. For the upper curves, there is less sensitivity to the emission angles because both the rf fields and E_2 are large.
[16] L. K. Ang *et al.*, IEEE Trans. Plasma Sci. (to be published).